Two-dimensional charge transport in self-organized, high-mobility conjugated polymers

H. Sirringhaus[*], P. J. Brown[*], R. H. Friend[*], M. M. Nielsen[†], K. Bechgaard[†], B. M. W. Langeveld-Voss[‡], A. J. H. Spiering[‡], R. A. J. Janssen[‡], E. W. Meijer[‡], P. Herwig[§] & D. M. de Leeuw[§]

[*] *Cavendish Laboratory, University of Cambridge, Madingley Road, Cambridge CB3 0HE, UK*
[†] *Condensed Matter Physics and Chemistry Department, Risø National Laboratory, 4000 Roskilde, Denmark*
[‡] *Laboratory of Macromolecular and Organic Chemistry, Eindhoven University of Technology, 5600 MB Eindhoven, The Netherlands*
[§] *Philips Research Laboratories, Prof. Holstlaan 4, 5656 AA Eindhoven, The Netherlands*

Self-organization in many solution-processed, semiconducting conjugated polymers results in complex microstructures, in which ordered microcrystalline domains are embedded in an amorphous matrix[1]. This has important consequences for electrical properties of these materials: charge transport is usually limited by the most difficult hopping processes and is therefore dominated by the disordered matrix, resulting in low charge-carrier mobilities[2] ($\leqslant 10^{-5}$ cm^2 V^{-1} s^{-1}). Here we use thin-film, field-effect transistor structures to probe the transport properties of the ordered microcrystalline domains in the conjugated polymer poly(3-hexylthiophene), P3HT. Self-organization in P3HT results in a lamella structure with two-dimensional conjugated sheets formed by interchain stacking. We find that, depending on processing conditions, the lamellae can adopt two different orientations—parallel and normal to the substrate—the mobilities of which differ by more than a factor of 100, and can reach values as high as 0.1 cm^2 V^{-1} s^{-1} (refs 3, 4). Optical spectroscopy of the field-induced charge, combined with the mobility anisotropy, reveals the two-dimensional interchain character of the polaronic charge carriers, which exhibit lower relaxation energies than the corresponding radical cations on isolated one-dimensional chains. The possibility of achieving high mobilities via two-dimensional transport in self-organized conjugated lamellae is important for applications of polymer transistors in logic circuits[5] and active-matrix displays[4,6].

We have studied the microstructure of 70–100 nm, spin-coated, regioregular P3HT films by grazing-incidence X-ray diffraction (XRD) on parts of the same SiO$_2$/Si substrates on which field-effect transistor (FET) devices were fabricated. Regioregularity denotes the percentage of stereoregular head-to-tail (HT) attachments of the hexyl side chains to the 3-position of the thiophene rings[7]. Two different orientations of the microcrystalline P3HT domains with respect to the FET substrate have been identified (Fig. 1). They are evident from the different intensity distributions of the (100) reflections due to the lamella layer structure and the (010) reflections due to π–π interchain stacking[8]. In samples with high regioregularity (>91%) and low molecular weight the preferential orientation of ordered domains is with the (100)-axis normal to the film and the (010)-axis in the plane of the film (Fig. 1a). In contrast, in samples with low regioregularity (81%) and high molecular weight, the crystallites are preferentially oriented with the (100)-axis in the plane and the (010)-axis normal to the film (Fig. 1b)[9]. The cause of this surprising change of orientation is not fully understood. It must be a dynamic phenomenon during the rapid growth of spin-coated films affected by either regioregularity or molecular weight. In films prepared by slow casting from a dilute solution the (100)-axis is normal to the film for all polymers (green trace in Fig. 1c and d).

However, the ability to induce different orientations allows us to establish a direct correlation between the direction of π–π stacking and the in-plane FET mobility μ (Fig. 2a). At room temperature the highest mobilities of 0.05–0.1 cm^2 V^{-1} s^{-1} are observed for the sample with the highest regioregularity (96%) and the largest size of crystallites with in-plane orientation of the (010)-axis (~95 Å, as estimated from (010) line shape analysis[10]). For spin-coated samples with HT ≈ 81%, in which the (010)-axis is normal to the film, the mobility is only 2×10^{-4} cm^2 V^{-1} s^{-1} in spite of pronounced in-plane crystallinity along the (100)-axis with a grain size of 130 Å. No clear correlation between FET mobility and weight average molecular weight M_w could be established, as seen previously between conductivity and M_w in highly doped P3HT (ref. 11). This is consistent with the FET mobility being limited by π–π interchain rather than intrachain transport as discussed below. In the case of the low-regioregularity polymers it is possible to directly compare mobilities for the in-plane (cast films) and out-of-plane orientation (spin-coated films) of the π–π stacking direction (Fig. 1d). In cast films of the 81% polymer the mobility is higher by more than an

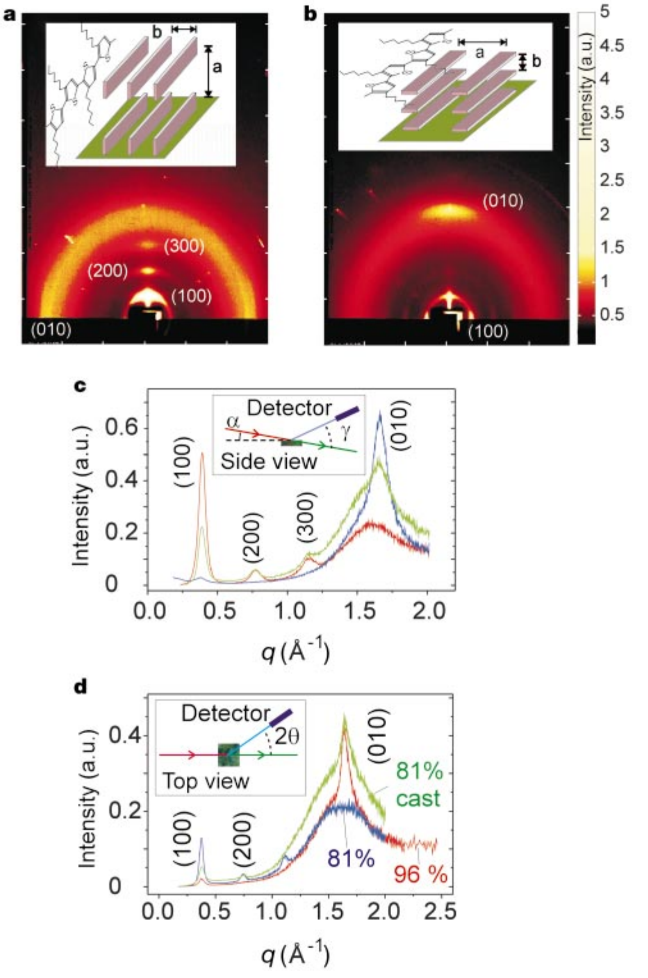

Figure 1 Two different orientations of ordered P3HT domains with respect to the FET substrate. **a**, **b**, The wide-angle X-ray scattering images are a colour representation of the two-dimensional distribution of scattered Cu Kα X-ray intensity from spin-coated, 70–100 nm thick P3HT films with regioregularity of 96% (**a**) and 81% (**b**) on SiO$_2$/Si substrates. The vertical (horizontal) axes correspond to scattering normal (parallel) to the plane of the film. The insets show schematically the different orientations of the microcrystalline grains with respect to the substrate. **c**, **d**, The change of orientation is confirmed by high-resolution synchrotron X-ray diffraction measurements for constant, grazing-incidence angle with out-of-plane (**c**) and in-plane (**d**) scattering geometry. Red, 96%, spin coated; blue, 81%, spin coated; green, 81%, solution-cast. The intensities plotted versus the total scattering vector are corrected for polarization and geometric factors[10].

order of magnitude than in spin-coated samples and only slightly lower than that of the highly regioregular polymers (Fig. 2a).

The large mobility anisotropy caused by different preferential orientations of the ordered, microcrystalline domains is clear evidence that the transport is no longer dominated by the remaining amorphous regions of the polymer film but is starting to reflect the transport properties of charge carriers in ordered polymer domains. The highest mobilities of 0.1 $\mathrm{cm^2\,V^{-1}\,s^{-1}}$ and the mobility anisotropy for in- and out-of-plane π–π stacking of $\sim$100 are of the same order of magnitude as in di-hexyl sexithiophene oligomer single crystals[12]. The residual disorder in the films manifests itself in a thermally activated mobility at low temperatures (Fig. 2b). This is interpreted in terms of a distribution of disorder-induced, deeply localized states below the high-mobility electronic states at which charge transport occurs. The activation energies E_a extracted between room temperature and 150 K ($\mu \propto \exp(-E_a/kT)$) are comparable for the different polymers ($E_a = 84$ meV (96%), 100 meV (95%), 115 meV (81%)) suggesting similar degrees of disorder. From our experiments, the intrinsic mobility limit of a hypothetical P3HT single crystal cannot be estimated. However, we have entered a transport regime, in which at room temperature and high gate voltages the Fermi level at the interface is sufficiently close to the charge transport level that intrinsic transport effects such as mobility anisotropies reflecting local polymer self-organization can be observed.

We conclude that the high mobilities of 0.1 $\mathrm{cm^2\,V^{-1}\,s^{-1}}$ reported recently[3,4] for the parallel orientation reflect efficient interchain transport in the two-dimensional conjugated lamellae. We discuss how these strong π–π interchain interactions may affect the nature of the charge-carrying species. Charge carriers in disordered polymers can be regarded as molecular radical cations formed on isolated, finite conjugated segments of the chain between two conjugation defects[13]. Due to polaronic relaxation of the local electronic and lattice structure the energy levels of a radical cation are shifted relative to those of the neutral molecule, giving rise to additional optical transitions upon charge injection (Fig. 3a). Charge modulation spectroscopy (CMS) measures changes of the optical transmission of a semitransparent FET upon gate-voltage induced modulation of the charge carrier density in the accumulation layer. It yields direct spectroscopic information about the charge carriers in polymer FETs (refs 14, 15) without the disturbing effects of counterions that are present in chemical doping experiments. The CMS spectra clearly show charge-induced, sub-gap transitions giving direct evidence for the polaronic nature of the charge carriers. For 81% (96%) samples we observe a strong transition at 1.70 eV (1.75 eV), a second transition appearing as a shoulder at 1.35 ± 0.05 eV (Fig. 3a), and a third transition at 0.35 eV (0.32 eV) in the mid-infrared spectral range (Fig. 3b). The associated bleaching—that is, reduction of the strength of the π–π^* absorption ($\Delta T/T > 0$)—of those chains on which the charges are located (Fig. 3a) exhibits pronounced vibronic structure, which is more structured and red-shifted compared to the inhomogeneously broadened absorption spectrum of the film (P.J.B., H.S. and R.H.F., manuscript in preparation). This shows that the charge carriers observed in CMS have migrated to the most ordered domains in the film; this allows us to claim that the CMS spectra reported here yield the intrinsic spectroscopic signature of charge carriers in ordered P3HT domains. This is further corroborated by the observation that the CMS spectra in the visible and near-infrared exhibit no significant dependence of the relative intensities, energies, or the number of transitions on temperature T (100–300 K), modulation frequency, and carrier density (P.J.B., H.S. and R.H.F., manuscript in preparation). Therefore, the observed charge-induced transitions must belong to the same physical species, in contrast to CMS studies on oligothiophenes[15] and less-ordered P3HT (ref. 14), in which there is coexistence of singly-charged radical cations, and doubly-charged dications and π-dimers. The observation of just one type of carrier in self-organized P3HT FETs is a manifestation of the low density of chemical and structural defects that may stabilize other carriers. From the independence of the CMS spectra with respect to temperature and charge carrier density we conclude that the carriers are singly-charged. Doubly-charged carriers would tend to dissociate at high temperatures and low carrier densities[16].

In order to identify the spectroscopic signature of interchain interaction effects we compare the CMS spectra of P3HT FETs with chemical doping experiments on isolated oligo- and polythiophene radical cations ($\mathrm{nT^+}$) in solution[16,17]. For $\mathrm{nT^+}$ two characteristic optical transitions, C1 and C2, are observed. Their energy red-shifts monotonically with increasing conjugation length (Fig. 3a). A third transition C3 is symmetry-forbidden on isolated chains[16] and is not observed in the $\mathrm{nT^+}$ spectra. The CMS spectra of self-organized P3HT presented here reveal characteristic features that cannot be understood as an extrapolation of the $\mathrm{nT^+}$ radical cation spectra to long conjugation lengths: (1) We observe three transitions at 0.3–0.35 eV, 1.35 eV and 1.75 eV, the strongest of which (at 1.75 eV) is at significantly higher energy E than the charge-induced transitions of isolated $\mathrm{nT^+}$. It blue-shifts towards the π–π^* transition with increasing regioregularity ($\Delta E \approx 50$ meV between 81% and 96%)

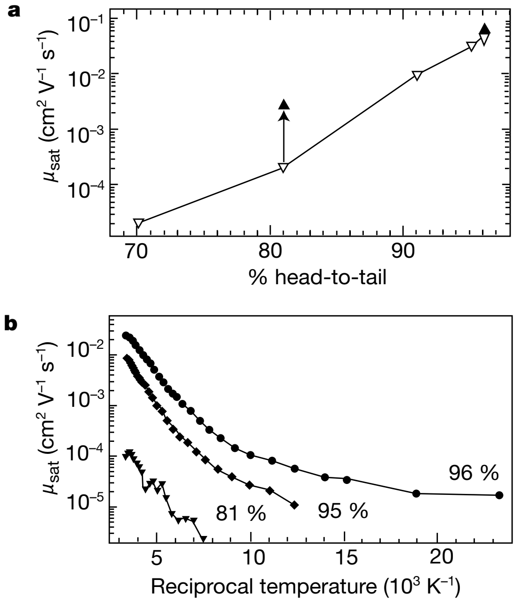

Figure 2 Charge carrier mobility of P3HT field-effect transistors with different microstructures. **a**, Dependence of the room-temperature mobility on the regioregularity for spin-coated (downward triangles) and solution-cast (upward triangles) top-contact P3HT FETs (channel length $L = 75\,\mu$m, channel width $W = 1.5$ mm). **b**, Temperature dependence of the field-effect mobility extracted from the characteristics of spin-coated bottom-contact P3HT FETs in the saturation regime ($L = 10\,\mu$m, $W = 3$ mm). Measurements were performed in vacuum ($p < 1 \times 10^{-6}$ mbar) to prevent charge trapping by adsorbed atmospheric impurities. The mobility of top-contact FETs with Au source–drain contacts evaporated after deposition of the polymer is higher, typically by a factor of two, than that of bottom-contact devices[4].

whereas the infrared transition at ~0.35 eV red-shifts. (2) Below ~0.3 eV we observe low-energy transitions (CT) extending into the energy range of sharp charge-induced, vibrational 'amplitude modes' (AM)[18]. The intensity of the low-energy CT feature increases with regioregularity. Their overlap with the AM results in a sharp dip at 0.18 eV, which may be due to a Fano-type resonance caused by interactions of a discrete level with a continuum[19]. (3) The charge-induced transitions exhibit no vibronic structure in contrast to those of isolated oligomers, while at the same time the associated bleaching signal has a pronounced vibronic structure.

We regard these three characteristic features, not present in isolated radical cation spectra, as an experimental determination of the spectroscopic signature of the two-dimensional nature of charge carriers in the two-dimensional conjugated lamellae of ordered P3HT. In the presence of strong π–π interchain interactions, for which the microstructure–mobility correlation gives clear evidence, the carriers should no longer be confined to a single chain. Although the carriers still have a polaronic nature, requiring their wavefunctions to be localized, they have a pronounced interchain character, with wavefunctions spreading over neighbouring chains[20,21]. This provides an explanation for the observed shift of the energy levels towards the highest occupied (π) and lowest unoccupied (π^*) molecular orbitals (Fig. 3a), reflecting a lowering of the polaronic relaxation energy. The transitions at 0.35 eV, 1.35 eV and 1.75 eV may be related to the C1, C2 and C3 transitions, respectively, of the one-electron model of isolated radical-cations (Fig. 3a, $C1 + C2 \approx C3$). It has been suggested that, in the presence of interchain interactions, transitions such as C3 (that are symmetry-forbidden in isolated molecules) may become intense[21]. However, for a full theoretical understanding of the spectra a proper treatment of interchain and electron–electron interactions will be required. In the case of small relaxation energies and strong interchain interactions one may expect that due to configuration interactions[16] charge-transfer like transitions (CT in Fig. 3) may become intense. They may explain the intense infrared absorption <0.3 eV.

The evidence for an association of high-mobility with two-dimensional charge transport provides a firm basis for exploring supramolecular self-organization to enhance charge transport in conjugated polymer semiconductors. By better control of structural anisotropy, and by developing polymers with more strongly π–π interacting building blocks[22], even higher mobilities and, possibly, a truly delocalized transport regime may be reached. ☐

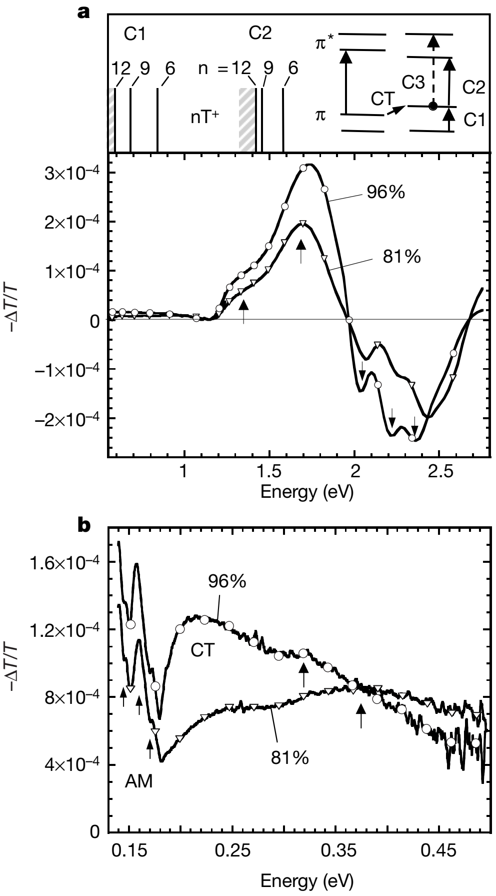

Figure 3 Charge modulation spectroscopy of semitransparent P3HT FETs in the accumulation regime. The devices were prepared under the same conditions and with similar mobilities as standard FETs and XRD samples (circles–96%, triangles–81%). **a**, **b**, The spectra show the fractional change of the optical transmission upon modulation of the gate voltage as a function of photon energy in the near-infrared and visible (**a**) and mid-infrared spectral range (**b**) ($T = 300$ K). Inset: schematic one-electron energy levels of neutral molecules and isolated radical cations, with the experimental energy value of the C1 and C2 transitions of nT^+ oligothiophene radical cations in solution (taken from ref. 16) shifting to lower energies with increasing n. In the solid state the transitions would be expected to be further red-shifted due to dielectric polarization effects. From the X-ray diffraction correlation lengths the conjugation length of the P3HT polymer is estimated to be $n \approx 20$–25.

Methods

Samples with HT regioregularity of 70% and 81% (molecular weight $M_w = 126$ kg mol^{-1} and 175 kg mol^{-1}, respectively; polydispersity $D = 2.5$–2.7) were synthesized by oxidative coupling with $FeCl_3$. Following the McCullough route, P3HT with regioregularity of 91% and 95% HT ($M_w = 11$ and 28 kg mol^{-1}, $D = 1.4$) was obtained. The highest regioregularity was a 96% HT sample synthesized by the Rieke route ($M_w = 28$ kg mol^{-1}, $D = 1.4$). For a review of the different synthesis routes see ref. 7. The regioregularity was determined by ^{1}H-NMR by comparing the signal intensities at 2.80 and 2.60 p.p.m. This yields a lower but more reliable value than analysis of the aromatic region of the spectrum. Films were spin-coated from a 0.8 weight % solution in $CHCl_3$ onto FET substrates (230 nm SiO_2 gate insulator on top of n^+-Si gate electrodes) treated with the silylating agent hexamethyldisilazane to promote self-organization.

X-ray diffraction measurements were performed under inert He atmosphere to minimize air scattering and beam damage. A grazing incidence angle below the critical angle of total reflection from the substrate, but above the critical angle for the film, was chosen to enhance the sensitivity to the thin polymer film. Synchrotron XRD measurements were performed at the BW2 beamline of the German electron synchrotron facility (DESY) in Hamburg.

Received 12 March; accepted 3 August 1999.

1. Samuelsen, E. J. & Mårdalen, J. in *Handbook of Organic Conductive Molecules and Polymers* Vol. 3 (eds Nalwa, H. S.) 87–120 (Wiley, Chichester, UK, 1997).
2. Kobashi, M. & Takeuchi, H. Inhomogeneity of spin-coated and cast non-regioregular poly(3-hexylthiophene) films. Structures and electrical and photophysical properties. *Macromolecules* **31,** 7273–7278 (1998).
3. Bao, Z., Dodabalapur, A. & Lovinger, A. J. Soluble and processable regioregular poly(3-hexylthiophene) for thin film field-effect transistor applications with high mobility. *Appl. Phys. Lett.* **69,** 4108–4110 (1996).
4. Sirringhaus, H., Tessler, N. & Friend, R. H. Integrated optoelectronic devices based on conjugated polymers. *Science* **280,** 1741–1744 (1998).
5. Drury, C. J., Mutsaers, C. M. J., Hart, C. M., Matters, M. & deLeeuw, D. M. Low-cost all-polymer integrated circuits. *Appl. Phys. Lett.* **73,** 108–110 (1998).
6. Dodabalapur, A. *et al.* Organic smart pixels. *Appl. Phys. Lett.* **73,** 142–144 (1998).
7. McCullough, R. D. The chemistry of conducting polythiophenes. *Adv. Mater.* **10,** 93–116 (1998).
8. Prosa, T. J., Winokur, M. J., Moulton, J., Smith, P. & Heeger, A. J. X-ray structural studies of poly(3-alkylthiophenes)—An example of an inverse comb. *Macromolecules* **25,** 4364–4372 (1992).
9. Fell, H. J., Samuelsen, E. J., Als-Nielsen, J., Grübel, G. & Mårdalen, J. Unexpected orientational effects in spin-cast, sub-micron layers of poly(alkylthiophene)s: A diffraction study with synchrotron radiation. *Solid State Commun.* **94,** 843–846 (1995).
10. Warren, B. E. *X-ray Diffraction* 41–50 (Addison-Wesley, Reading, USA, 1969).
11. Ishikawa, H. *et al.* Effect of molecular mass of poly(3-alkylthiophene) on electrical properties. *J. Phys. D* **25,** 897–900 (1992).
12. Schön, J. H., Kloc, C., Laudise, R. A. & Batlogg, B. Electrical properties of single crystals of rigid rodlike conjugated molecules. *Phys. Rev. B* **58,** 12952–12957 (1998).
13. Deussen, M. & Bässler, H. Anion and cation absorption spectra of conjugated oligomers and polymer. *Synth. Met.* **54,** 49–55 (1993).
14. Ziemelis, K. E. *et al.* Optical spectroscopy of field-induced charge in poly(3-hexyl thienylene) metal-insulator-semiconductor structures: Evidence for polarons. *Phys. Rev. Lett.* **66,** 2231–2234 (1991).
15. Harrison, M. G., Fichou, D., Garnier, F. & Yassar, A. *In situ* charge-modulation spectroscopy of oligothiophene field-effect diodes: from sexithiophene towards polythiophene. *Opt. Mater.* **9,** 53–58 (1998).
16. Haare, J. A. E. H. V. *et al.* Redox states of long oligothiophenes: Two polarons on a single chain. *Chem. Eur. J.* **4,** 1509–1522 (1998).
17. Horowitz, G., Yassar, A. & Bardeleben, H. J. V. ESR and optical spectroscopy evidence for a chain

length dependence of the charged states of thiophene oligomers. Extrapolation to polythiophene. *Synth. Met.* **62,** 245–252 (1994).
18. Horovitz, B. Infrared activity of Peierls systems and application to polyacetylene. *Solid State Commun.* **41,** 729–734 (1982).
19. Fano, U. Effects of configuration interaction on intensities and phase shifts. *Phys. Rev.* **124,** 1866–1878 (1961).
20. Emin, D. Self-trapping in quasi-one-dimensional solids. *Phys. Rev. B* **33,** 3973–3975 (1986).
21. Blackman, J. A. & Sabra, M. K. Interchain coupling and optical absorption in degenerate and nondegenerate polymers. *Phys. Rev. B* **47,** 15437–15448 (1993).
22. Sirringhaus, H. *et al.* Bis(dithienothiophene) organic field-effect transistors with a high ON/OFF ratio. *Appl. Phys. Lett.* **71,** 3871–3873 (1997).

Acknowledgements

We thank J. Cornil, D. Dos Santos, and A. J. Flewitt for contributions. Financial support from the European Commission and the Training and Mobility of Researchers (TMR) programme is acknowledged. H.S. thanks the Royal Society for a University Research Fellowship.

Correspondence and requests for materials should be addressed to H.S. (e-mail: hs220@phy.cam.ac.uk).

Identifying magma–water interaction from the surface features of ash particles

Ralf Büttner*, Pierfrancesco Dellino† & Bernd Zimanowski*

* *Physikalisch Vulkanologisches Labor, Institut für Geologie, Universität Würzburg, Pleicherwall 1, D-97070 Würzburg, Germany*
† *Dipartimento Geomineralogico, Universitá degli Studi di Bari, Via Orabona 4, 1-70125 Bari, Italy*

The deposits from explosive volcanic eruptions (those eruptions that release mechanical energy over a short time span[1]) are characterized by an abundance of volcanic ash[2,3]. This ash is produced by fragmentation of the magma driving the eruption and by fragmenting and ejecting parts of the pre-existing crust (host rocks). Interactions between rising magma and the hydrosphere (oceans, lakes, and ground water) play an important role in explosive volcanism[4,5], because of the unique thermodynamic properties of water that allow it to very effectively convert thermal into mechanical energy. Although the relative proportion of magma to host-rock fragments is well preserved in the pyroclastic rocks deposited by such eruptions, it has remained difficult to quantitatively assess the interaction of magma with liquid water from the analysis of pyroclastic deposits[2–5]. Here we report the results of a study of natural pyroclastic sequences combined with scaled laboratory experiments. We find that surface features of ash grains can be used to identify the dynamic contact of magma with liquid water. The abundance of such ash grains can then be related to the water/magma mass ratios during their interaction.

From direct observation of 'wet' volcanic eruptions (phreatomagmatic eruptions) and the analysis of their deposits, several criteria have been defined that qualitatively indicate the presence of liquid water during an eruption[2,3,6,7]. The reconstruction of volcanic eruptions from their deposits, however, would benefit from a tool that could quantitatively indicate the amount of liquid water that encountered the magma. A perfect laboratory volcano for investigations of magma–water contact is the active Italian volcanic island of Vulcano and its young crater, La Fossa, where various kinds of phreatomagmatic deposits, spanning the range of water–magma phenomenologies reported in the literature, are present.

Phreatomagmatic deposits at La Fossa di Vulcano have formed during almost all of the numerous eruptions characterizing its volcanic history, which started ~6,000 years ago, with the last eruption being the 'vulcanian' one of AD 1888–1890 (ref. 8). Following the scheme used in the literature[9–11], these deposits have been subdivided into two categories: 'wet' and 'dry' surge deposits, both being the products of laterally moving surges of low-density ash clouds. The difference between the two types is evidenced by their structural and textural features. 'Dry'-type deposits are decimetres to metres thick densely laminated layers of coarse ash and lapilli; 'wet'-type deposits are mostly not internally structured (that is, "massive") centimetres thick fine-ash layers with features such as accretionary lapilli, vesiculated tuff, and plastic type deformation[7].

Various structures of deposits have been interpreted using results from early magma–water interaction experiments[12]. In 'dry' explosions the interaction is suggested to be more effective, with all water consumed during interaction and transformed into superheated steam, whereas in 'wet' explosions, the interaction is less effective,

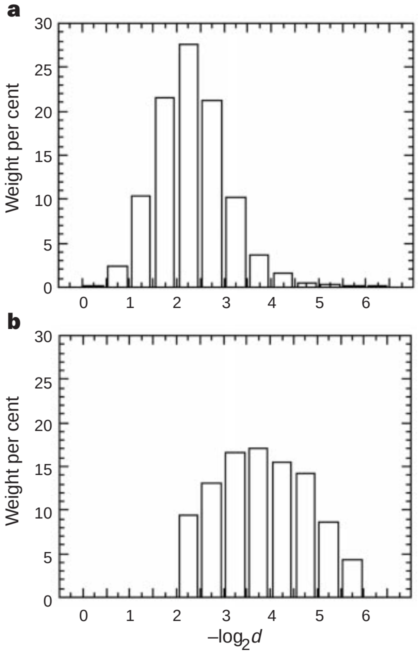

Figure 1 Grain size distribution of phreatomagmatic deposits of La Fossa di Vulcano. The figures show the proportional importance of grain size fractions in weight per cent (*d* is the sieve mesh size in millimetres). **a**, Histogram of a representative 'dry' surge deposit. **b**, Histogram of a representative 'wet' surge deposit.